Solid State Sciences 13 (2011) 66–71

Contents lists available at ScienceDirect

Solid State Sciences

journal homepage: www.elsevier.com/locate/ssscie

Characterization, photoluminescence, thermally stimulated luminescence and electron spin resonance studies of Eu^{3+} doped $LaAlO_3$ phosphor

Vijay Singh [a,*], S. Watanabe [b], T.K. Gundu Rao [b], J.F.D. Chubaci [b], Ho-Young Kwak [a,*]

[a] Mechanical Engineering Department, Chung-Ang University, Seoul 156-756, Republic of Korea
[b] Institute of Physics, University of Sao Paulo, 05508-090 Sao Paulo/SP, Brazil

ARTICLE INFO

Article history:
Received 15 February 2009
Received in revised form
17 August 2010
Accepted 22 October 2010
Available online 29 October 2010

Keywords:
Luminescence
Doping
Phosphors
ESR
TSL
Defect centres
Europium

ABSTRACT

Europium-doped lanthanum aluminate ($LaAlO_3$) powder was prepared by using a combustion method. The crystallization, surface morphology, specific surface area and luminescence properties of the samples have been investigated. Photoluminescence studies of Eu doped $LaAlO_3$ showed orange-reddish emission due to Eu^{3+} ions. $LaAlO_3$:Eu^{3+} exhibits one thermally stimulated luminescence (TSL) peak around 400 °C. Room temperature electron spin resonance spectrum of irradiated phosphor appears to be a superposition of two centres. One of them (centre I) with principal *g*-value 2.017 is identified as an O^- centre while centre II with an isotropic *g*-value 2.011 is assigned to an F^+ centre (singly ionized oxygen vacancy). An additional defect centre observed during thermal annealing around 300 °C grows with the annealing temperature. This centre (assigned to F^+ centre) originates from an F-centre (oxygen vacancy with two electrons) and the F-centre along with the associated F^+ centre appear to correlate with the observed TSL peak in $LaAlO_3$:Eu^{3+} phosphor. The activation energy for this peak has been determined to be 1.54 eV from TSL data.

1. Introduction

There is an increasing demand for economically viable phosphor materials. Rare-earth (RE) doped red/orange emitting phosphors are important as display device phosphors with on-going technological advancements. Hence optical properties of RE-doped crystals and glasses have been studied in detail [1–3]. Rare-earth ions (Eu^{3+}, Sm^{3+}, Tb^{3+}, etc.) have been widely used as luminescent centres in phosphor materials due to their sharp 4f-intra shell transitions [4–6].

Recently, optical properties of the trivalent europium (Eu^{3+}) doped crystals and glasses have been studied by several research groups. They have investigated Eu^{3+} emission in borates [7], oxides [8], silicates [9], phosphates [10], sulphates [11], fluorides [12], etc. Buddhudu et al. [13–16] synthesized and characterized certain Eu^{3+} doped powder phosphors in order to obtain red/reddish-orange fluorescence. Some of these compositions were for their use in the production of screens pertaining to display applications. It is our main interest to synthesise yet another family of newly developed Eu^{3+} doped aluminate phosphors via low temperature initiated combustion process and investigate their photoluminescence properties in view of the commercial importance of reddish-orange colour emitting phosphors.

It is well known that the defects in a material play a key role in the luminescence process and modulate the afterglow properties quite significantly. To gain a complete insight into the trapping mechanism, TSL and ESR analysis are widely used as an effective tool. In the present work, lanthanum aluminate ($LaAlO_3$) was chosen as a host material since it has a reasonably larger band gap of over 5 eV, and a high thermal stability up to 2100 °C [17]. Moreover, $LaAlO_3$ heterointerface has been the subject of intensive research in recent years [18,19]. Kuo et al. [20] investigated the phase transformation and crystallization kinetics of $LaAlO_3$ nanopowders. Chemical and structural characterizations of the $LaAlO_3$ (110) surface were investigated by Mortada et al. [21]. Recently, Singh et al. [22] reported the optical properties of $LaAlO_3$:Ho^{3+} phosphor. More recently, Dereń et al. [23] studied multiphonon transitions in $LaAlO_3$ doped with rare-earth ions. It was noticed that very few reports are available on impurities doped lanthanum aluminate ($LaAlO_3$) prepared by combustion method. There is no report on the identification of the radiation-induced defect centres formed on irradiation and the subsequent electron–hole recombination reactions resulting in the glow peaks. In view of this,

* Corresponding authors.
E-mail addresses: vijayjiin2006@yahoo.com (V. Singh), kwakh@cau.ac.kr (H.-Y. Kwak).

1293-2558/$ – see front matter © 2010 Elsevier Masson SAS. All rights reserved.
doi:10.1016/j.solidstatesciences.2010.10.010

we have carried out thermally stimulated luminescence (TSL) and electron spin resonance (ESR) investigations on gamma irradiated $LaAlO_3:Eu^{3+}$ phosphor. Finally based on ESR results we have suggested a most probable mechanism for the observed TSL peak. In addition, the prepared sample was characterized by X-ray diffraction (XRD), scanning electron microscopy (SEM), Brunauer–Emmet–Teller (BET) surface area and photoluminescence techniques.

2. Experimental

The method of preparation adopted for this work is combustion synthesis. Analytical grade $Al(NO_3)_3\cdot 9H_2O$, $La(NO_3)_3\cdot 6H_2O$, Eu_2O_3 and urea were used as the starting materials. For the combustion, metal nitrates as oxidizers, urea is employed as fuel and europium as dopant were used. The oxidizer:fuel ratio was calculated based on oxidizing (O) and fuel (F) valencies of the reactants, keeping O/F = 1, as reported earlier [22]. The energy released due to the exothermic reaction between the metal nitrates and urea can rapidly heat the system to high temperatures without an external heat source. Europium-doped lanthanum aluminate phosphor with the composition $La_{0.96}Eu_{0.04}AlO_3$ was prepared for the present investigations. The precursor chemicals were mixed in a China dish with a minimum quantity of de-ionized water to form a solution. The solution was introduced into a pre-heated furnace which was maintained at 500 ± 20 °C. Combustion took place with the introduction of the solution along with the evolution of gases. The solution was allowed to froth and swell thus forming foam, which ruptured with a flame and glowed to incandescence. During incandescence, the foam further swelled to the capacity of the container. The entire combustion process was over in less than 5 min. The dish was immediately removed from the furnace. The voluminous product was crushed into fine powder using pestle and mortar and was used for characterization.

Powder X-ray diffraction study was performed on a Philips X-ray diffractometer with graphite monochromatized CuK_α radiation ($\lambda = 0.15418$ nm) in the 2θ range of 15–80°. Photoluminescence measurements were carried out using a Hitachi F-4000 spectrofluorimeter at room temperature. The measurements of BET specific surface areas of samples were performed at 77 K by N_2 adsorption (Quantachrome, Autosorb 3a) after pre-treating them at over 200 °C for 1 h to remove adsorbed water. The morphology of the powders was obtained using a Hitachi S-4300 scanning electron microscope (SEM).

Samples were irradiated with a ^{60}Co gamma source. Daybreak 1100 series automated TL reader system (heating rate of 5 °C/s) was utilised for TSL experiments which were carried out in a nitrogen atmosphere. Electron Spin Resonance experiments were carried out on a Bruker EMX ESR spectrometer operating at X-band frequency with 100 kHz modulation frequency. Diphenyl Picryl Hydrazyl (DPPH) was used for calibration of *g*-values of defect centres. Temperature dependence of the ESR spectra was studied using Bruker B VT 2000 variable temperature accessory.

3. Results and discussions

3.1. XRD, SEM, BET and PL studies

Fig. 1 shows the X-ray diffractogram of as-prepared $LaAlO_3:Eu^{3+}$ powders. The phase analysis demonstrates that $LaAlO_3:Eu^{3+}$ is hexagonal with unit cell dimensions: $a = 5.368$ Å and $c = 13.12$ Å. This is in good agreement with the standard JCPDS files (82-0478). In this phosphor, trivalent lanthanum ions are replaced by trivalent europium ions. Dopant ions (Eu^{3+}) have no noticeable effect on the obtained X-ray diffractogram of the as-prepared $LaAlO_3:Eu^{3+}$ phosphor.

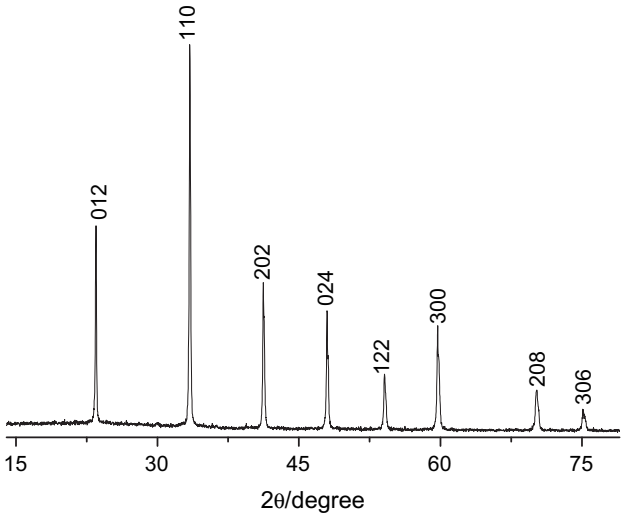

Fig. 1. X-ray diffractogram of $LaAlO_3:Eu^{3+}$ phosphor powder.

Surface features of the as-prepared $LaAlO_3:Eu^{3+}$ powder was studied using SEM. Fig. 2A–C presents SEM images of the powder under various magnifications. SEM image at low magnification, as shown in Fig. 2A, indicates that the crystallites have no uniform shapes and sizes. This non-uniformity of shape and size is due to the non-uniform distribution of temperature and mass flow in the combustion flame. Portion (a) of Fig. 2A is magnified to obtain Fig. 2B. Similarly portion (b) of Fig. 2B is magnified to obtain Fig. 2C. These high magnification SEM images show that there are several pores which are formed by the escaping gases during the combustion reaction. Also several small particles can be seen within grains. It may be mentioned that the observed features are inherent in combustion derived powders [24,25].

The BET specific surface area, total pore volume and average pore radius for the Eu^{3+} doped $LaAlO_3$ was found to be 5.5980 $m^2\,g^{-1}$, 21.2790 $ml\,g^{-1}$ and 71.2521 Å respectively. Patil et al. [26] reported that the specific surface areas of $LaAlO_3$ material prepared by the urea process to be 3.00 $m^2\,g^{-1}$. Europium doping did not significantly alter these results. Cimino et al. [27] have reported surface areas in the 4–33 $m^2\,g^{-1}$ range for $LaAl_{1-x}Mn_xO_3$ ($x = 0.0$–1.0) and they synthesized materials by the citrate method and calcined at 800 °C. It was found that surface area in the present system is higher as compared to pure lanthanum aluminate reported by Cimino et al.

Among the rare-earth ions, europium is an attractive activator and has been used in phosphor materials for an efficient red and blue emission. The europium emission in the phosphor material is strongly dependent on the host lattice and it is possible to obtain different colors from blue to red. Europium can act as an activator in two forms, viz. Eu^{2+} and Eu^{3+}. Eu^{3+} or Eu^{2+} can be identified from their characteristic photoluminescence spectrum. Dereń and Krupa [28] investigated absorption and emission spectra and observed Eu^{3+} emission in $LaAlO_3$ crystal. Later Eu^{3+} emission in $LaAlO_3$ nanocrystals has been reported by Hreniak et al. [29]. They have discussed in detail the mechanism of luminescence decay of Eu^{3+} ions in $LaAlO_3$ host. Recently, a mixed emission consisting of both band-emission of Eu^{2+} and line-emission of Eu^{3+} in $LaAlO_3$ has been reported by Mao et al. [30]. Fig. 3 shows the excitation (a) and emission (b) spectra of $LaAlO_3:Eu^{3+}$ phosphor prepared by the combustion method. The excitation spectrum of the $LaAlO_3:Eu^{3+}$ sample was monitored at 591 nm. The excitation spectrum (Fig. 3(a)) consists of a broad band ranging from 200 to 370 nm with a maximum at around 327 nm and some sharp lines in

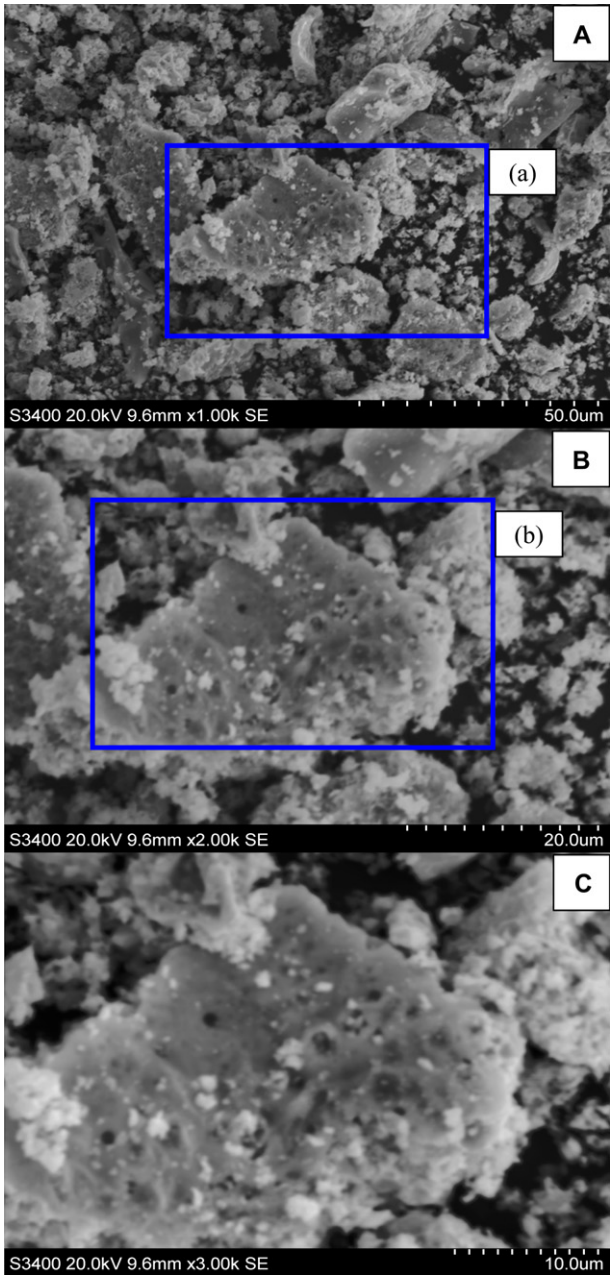

Fig. 2. SEM micrographs of $LaAlO_3:Eu^{3+}$ phosphor.

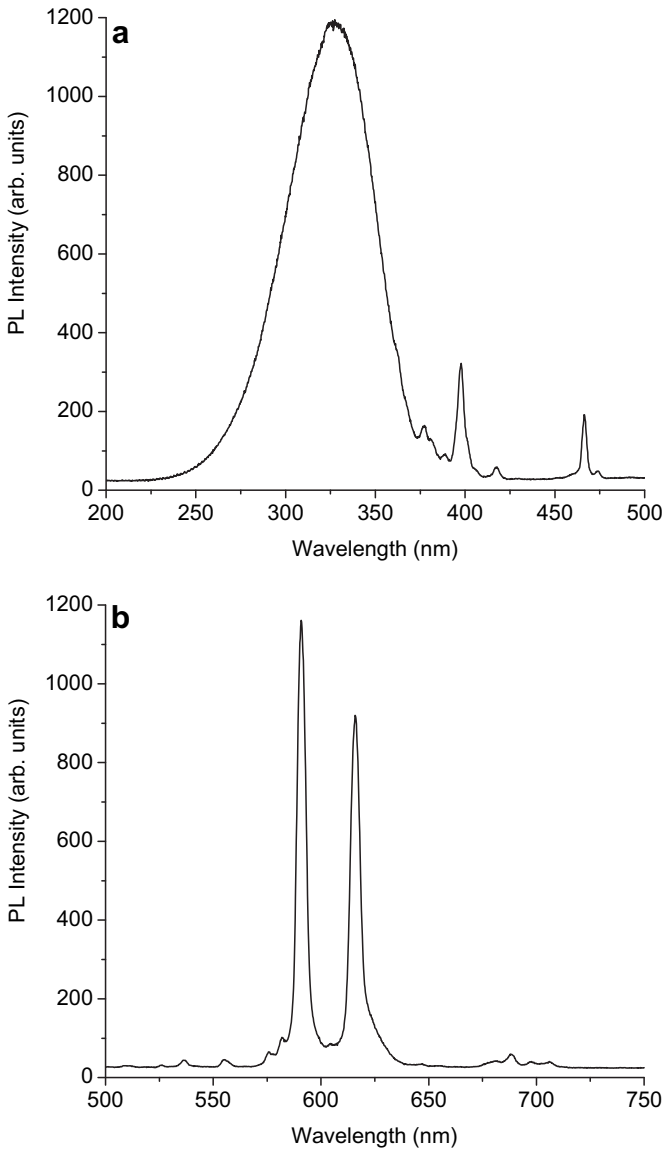

Fig. 3. Photoluminescence spectra of Eu^{3+} doped $LaAlO_3$, (a) excitation spectrum ($\lambda_{em} = 591$ nm), (b) emission spectrum ($\lambda_{ex} = 327$ nm).

the longer wavelength region. The dominant band at 327 nm may be due to the Eu^{3+}–O^{2-} charge transfer. The sharp lines in the longer wavelength region can be attributed to f–f transitions. The lines around 397 nm ($^7F_0 \rightarrow {}^5L_6$) and 466 nm ($^7F_0 \rightarrow {}^5D_2$) are the most noticeable.

The emission spectrum of $LaAlO_3:Eu^{3+}$ phosphor excited at 327 nm is shown in Fig. 3(b). There are peaks which are attributed to $^5D_0 \rightarrow {}^7F_J$ transitions indicating the existence of Eu^{3+} ions in the $LaAlO_3$ host. In the present case, the emission spectrum shows two strong sharp peaks at the 591 nm and 616 nm corresponding to the magnetic dipole transition ($^5D_0$–$^7F_1$) and electric dipole transition ($^5D_0$–$^7F_2$) of Eu^{3+} emission respectively. Weak peaks are seen on either side of strong peaks. Earlier workers have also observed these peaks in the Eu doped $LaAlO_3$ host which substantiate the presence of Eu^{3+} ions [28,29]. The intensity ratio of 591 nm peak to 616 nm peak is a measure of asymmetry of the Eu^{3+} site in the host lattice [31]. Luminescence study shows that magnetic dipole transition ($^5D_0$–$^7F_1$) is prominent over the electric dipole transition ($^5D_0$–$^7F_2$), which has been attributed to occupancy of inversion symmetry site by more Eu^{3+} ions in Eu^{3+} doped $LaAlO_3$. If more Eu^{3+} ions have an occupancy at the inversion site, the emission intensity from the $^5D_0$–$^7F_1$ transition will be enhanced and the phosphor will primarily exhibit orange luminescence. In the present investigation, the intensity of $^5D_0$–$^7F_1$ is dominant over $^5D_0$–$^7F_2$ transition. It may be mentioned that a similar dominant behaviour of magnetic dipole transition ($^5D_0$–$^7F_1$) was observed for Eu doped $LaAlO_3$ host [28–30]. The orange-red emission of the prepared $LaAlO_3:Eu^{3+}$ phosphor indicates its probable utility for display applications.

3.2. TSL and ESR studies

Prior to gamma irradiation no glow peaks were observed in $LaAlO_3:Eu^{3+}$ phosphor. Upon gamma irradiation (dose: 5 Gy), the phosphor exhibited a broad glow curve consisting of a single

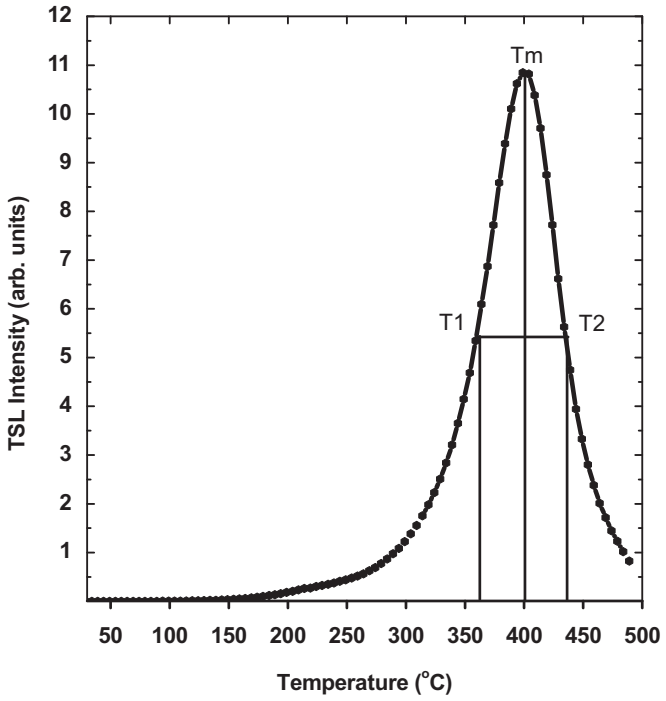

Fig. 4. TSL glow curve of $LaAlO_3:Eu^{3+}$ phosphor (gamma dose: 5 Gy).

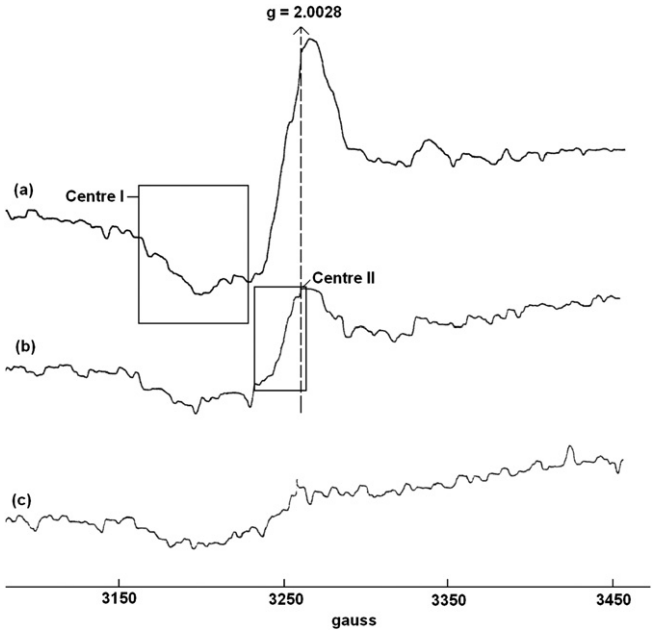

Fig. 5. Room temperature ESR spectra of irradiated $LaAlO_3:Eu^{3+}$ phosphor (gamma dose: 3000 Gy), (a) immediately after irradiation – line labeled as I is due to an O^- centre, (b) after annealing at 170 °C and (c) refers to spectrum recorded after annealing at 210 °C. Centre II line is assigned to an F^+ centre.

prominent peak around 400 °C (heating rate = 5 °C/s) (Fig. 4). Trapping parameters were calculated by using Chen's formulae [32] and are given in Table 1. The mean activation energy for the 400 °C glow peak of $LaAlO_3:Eu^{3+}$ was found to be 1.54 eV.

Fig. 5(a) shows the room temperature ESR spectrum of gamma irradiated (dose: 3 kGy) $LaAlO_3:Eu^{3+}$ phosphor. The observed spectrum appears to be a superposition of at least two distinct centres. This inference is based on thermal annealing experiments. These centres are labeled in Fig. 5(a) and (b). The ESR line labeled as I is due to a centre characterized by a single broad line with an isotropic *g*-value 2.017 and 59 gauss linewidth. Usually, not many defect centres are expected to be formed in a system like $LaAlO_3:Eu^{3+}$ and the most probable centres which can be observed are the V-centres, F-centres and F^+ centres.

Centre I has a large linewidth which indicates unresolved hyperfine structure. This is due to the interaction of the unpaired electron with nearby nuclear spins. Aluminum as well as lanthanum in $LaAlO_3$ have isotopes with nuclear spins 5/2, 5, 7/2: ^{27}Al, ^{138}La and ^{139}La. ^{27}Al is nearly as abundant (100%) as ^{139}La (99.9%) and its nuclear magnetic moment is slightly higher (3.6415) than that of ^{139}La (2.7832) [33]. It is likely, therefore, that the electronic spin will be interacting with aluminum ions and also possibly with lanthanum (^{139}La) ions. It is known that the cation disorder and non-stoichiometry of aluminates provide a large number of lattice defects which may serve as trapping centres. In such a case, oxygen vacancies should lead to F^+ centres by trapping electrons. On the other hand, hole trapping at aluminum and lanthanum vacancies can lead to formation of O^- centres. The observed broad ESR line of centre I and the associated unresolved hyperfine structure indicates that the unpaired electron is delocalized and interacts with nearby aluminum/lanthanum nuclei. It has been speculated [34] that in oxides, the charges must be trapped near double (or more) charged defects in order for the charge to be delocalized, thus allowing it to interact with surrounding nuclei. Hence centre I is tentatively assigned to a O^- centre – a hole trapped on an oxygen ion adjacent to an Al-ion/La-ion vacancy. The observed positive *g*-shift of centre I is also in accordance with the expectations for an O^- centre. It may be mentioned that a similar centre observed in other aluminates like neutron irradiated $MgAl_2O_4$ [35], gamma irradiated $LiAlO_2$ [36] and $ZnAl_2O_4$ phosphor [37] has also been ascribed to an O^- centre.

Table 1
Trapping parameters of $LaAlO_3:Eu^{3+}$ exposed to gamma irradiation (dose:5 Gy).

T1 (K)	Tm (K)	T2 (K)	μg	Eτ (eV)	Eδ (eV)	Eω (eV)
635	673	708	0.47	1.52	1.57	1.55

Tm is the temperature corresponding to the maximum TSL intensity and T1 and T2 are temperature on either side of Tm corresponding to half peak intensity. μg is a geometrical factor, E is the activation energy, and other symbols are from Chen's formulae [32].

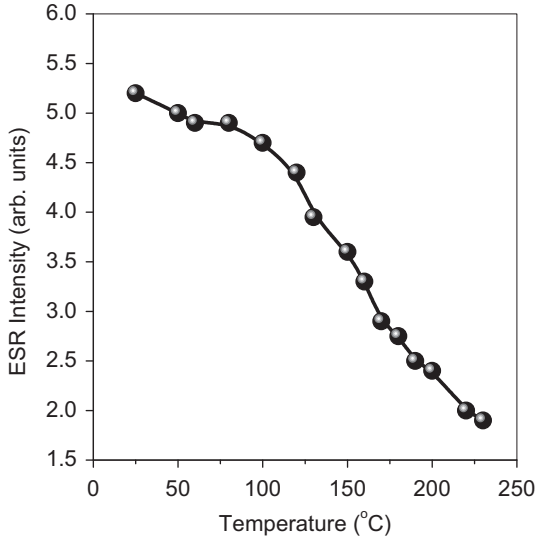

Fig. 6. Thermal annealing behaviour of centre I in $LaAlO_3:Eu^{3+}$ phosphor.

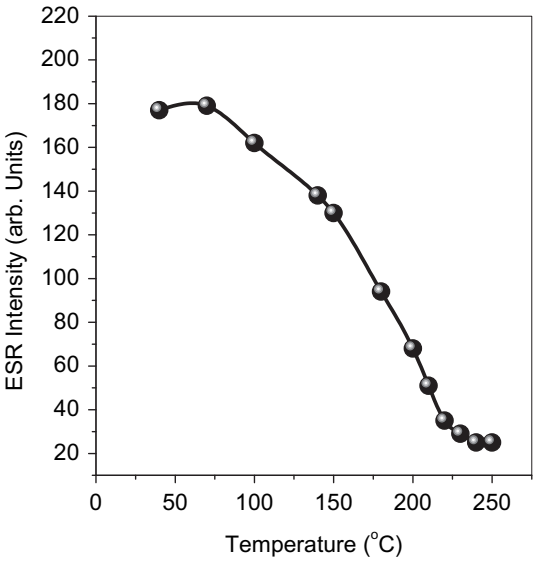

Fig. 7. Thermal annealing behaviour of centre II in $LaAlO_3:Eu^{3+}$ phosphor.

The stability of centre I was measured using the pulsed thermal annealing method. After heating the sample up to a given temperature value where it is maintained for 3 min, it is cooled rapidly down to room temperature for ESR measurements. The thermal annealing behaviour of centre I is shown in Fig. 6. It is observed that the centre decays at a relatively low temperature and does not relate to the observed TSL peak at 400 °C. It should be mentioned that there is an overlap of the relatively stronger centre II ESR line with centre I and the thermal annealing results shown in Fig. 6 is only a rough indicator of the decay behaviour of centre I.

The ESR line labeled as II in Fig. 5(b) is due to a centre characterized by a single ESR line with an isotropic *g*-value 2.011 and 29 gauss linewidth. One of the most probable centres which can be trapped in the present system is the F^+ centre (an electron trapped at an anion vacancy). Such a centre was first observed by Hutchison [38] in neutron irradiated LiF. Irradiation leads to the trapping of an electron at an anionic vacancy and such trapping is the basis for the formation of F^+ centres. Hyperfine interaction with the nearest-neighbor cations is the major contribution to the linewidth. Defect centre II formed in the present system is characterized by a small *g*-shift and the linewidth is reasonably large. The centre also does not exhibit any resolved hyperfine structure. On the basis of these observations and considerations of the characteristic features of the defect centres likely to be formed in a system such as $LaAlO_3:Eu^{3+}$, centre II is tentatively assigned to an F^+ centre. The thermal annealing behaviour of centre II is shown in Fig. 7 and it is seen that the centre decays completely around 230 °C.

From the thermal annealing experiments, it is seen that the two centres observed at room temperature decay at relatively low temperatures (below 230 °C). A careful examination of the ESR spectra of centre II during thermal annealing has shown a gradual appearance of a new centre (centre III). This centre appears as a relatively narrow line at around the same position as the centre II ESR line. A few relevant spectra showing the appearance, growth and decay of centre III are shown in Fig. 8. Centre III has an isotropic *g*-factor of 2.0035 with a 7 gauss linewidth and is tentatively assigned to an F^+ centre based on the reasons mentioned earlier. It may be mentioned that the E_1'-centre (an oxygen vacancy having an unpaired electron localized in the sp^3 hybrid orbital extending into the vacancy from the adjacent silicon ion) exhibits a similar formation behaviour in SiO_2. While investigating the formation and thermal annealing characteristics of E_1'-centre in SiO_2, Jani et al. [39] have observed that room temperature irradiation alone does not readily form E_1'-centres. It was found that the E_1'-centre concentration was enhanced by thermal annealing at high temperature following room temperature irradiation. A two-step process has been suggested by Jani et al. for the formation of E_1'-centre. The initial room temperature irradiation changes either the basic SiO_2 lattice or the precursor defects into an intermediate state. Subsequent thermal treatment at high temperature then converts this intermediate state into the E_1'-centre through the

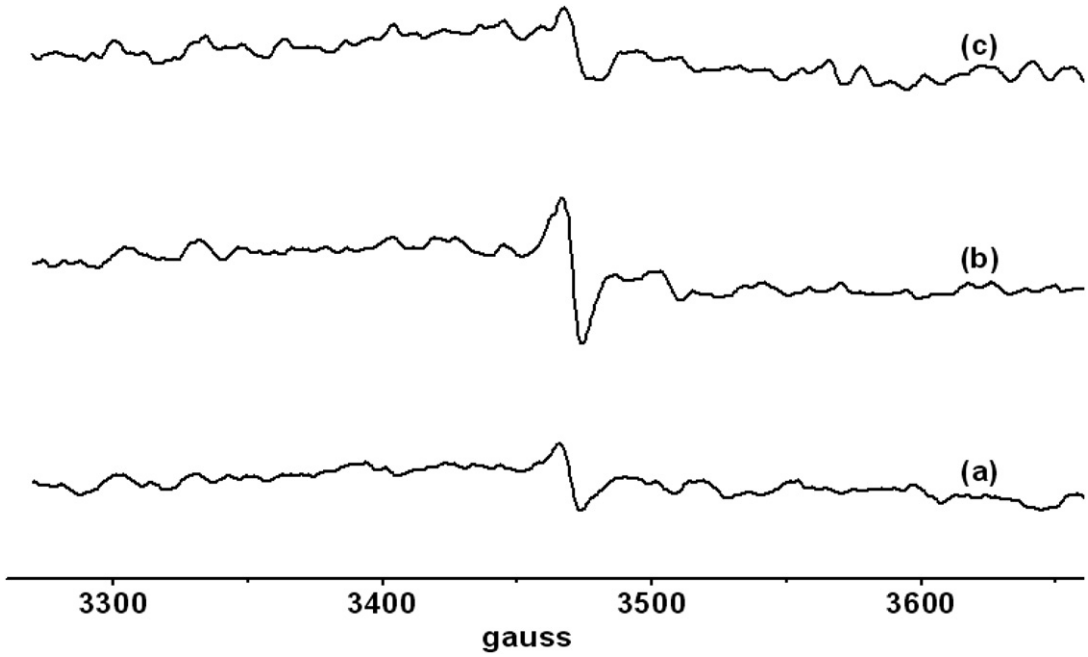

Fig. 8. ESR spectra of irradiated $LaAlO_3:Eu^{3+}$ phosphor after thermal anneal at high temperatures; (a), (b), and (c) correspond to thermal anneal at 320, 360 and 430 °C respectively. The spectra show the appearance, growth and decay of centre III (F^+ centre).

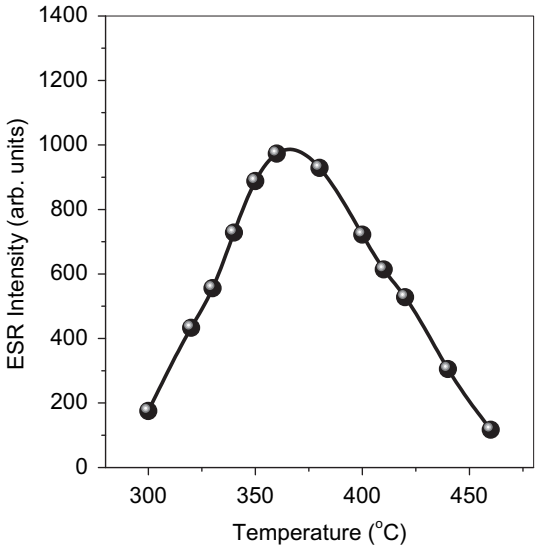

Fig. 9. Thermal annealing behaviour of centre III in $LaAlO_3:Eu^{3+}$ phosphor.

transfer of electrons. An oxygen vacancy containing two electrons in a singlet state ($S=0$) has been proposed by Jani et al. as the precursor of the E_1'-centre. They propose that this oxygen vacancy with two electrons is likely to release an electron during post-irradiation heating resulting in the formation of E_1'-centre. On the basis of these results in SiO_2, it is speculated that in $LaAlO_3:Eu^{3+}$ phosphor, the formation process of centre III might be similar.

As mentioned earlier, cation disorder and non-stoichiometry of aluminates like $LaAlO_3$ may provide native oxygen vacancies which can be converted into F-centres during room temperature irradiation. F-centre contains two electrons in a singlet state ($S=0$) and during heating releases an electron which appears in the thermal annealing experiments as a growth of centre III. This expectation is in accord with the thermal annealing behaviour of centre III which is shown in Fig. 9. It is seen that the centre grows in the temperature region 300–360 °C and the decay of the centre at high temperatures corresponds to the decay of F^+ centre. Taken in conjunction with the observed TSL peak at 400 °C, the present observations indicate that the precursor of centre III (F-centre) and also centre III (F^+ centre) together appear to correlate with the TSL peak in $LaAlO_3:Eu^{3+}$ phosphor. During thermal readout, the F-centre and also F^+-centre release an electron and the released electrons can combine with holes trapped elsewhere. The energy released in the electron–hole recombination process is used for the excitation of Eu^{3+} ion resulting in the TSL glow peak.

4. Conclusions

Eu^{3+} doped $LaAlO_3$ powder phosphor was prepared by urea combustion technique involving furnace temperatures of about 500 °C in a short time. The X-ray diffractogram analysis supports the Eu^{3+} substitution at La^{3+} without disturbing the $LaAlO_3$ crystal lattice. The major advantages of the combustion process are its simplicity, speed and lower cost. Further, the present results, though preliminary in nature, suggest that Eu^{3+} doped $LaAlO_3$ phosphors have the potential to be used as orange-red emitting phosphors for display devices. The $LaAlO_3:Eu^{3+}$ phosphor exhibits a single TSL glow peak around 400 °C. Several defect centres have been identified in irradiated phosphor. These centres are tentatively assigned to an O^- centre and F^+ centres. A neutral F-centre (oxygen vacancy with two electrons) and the associated F^+-centre appear to correlate with the 400 °C TSL peak.

References

[1] Amanda E. Henkes, Raymond E. Schaak, J. Solid State Chem. 181 (2008) 3264.
[2] N. Lakshminarasimhan, U.V. Varadaraju, Mater. Res. Bull. 43 (2008) 2946.
[3] Hucheng Yang, Chengyu Li, Ye Tao, Jianhua Xu, Guobin Zhang, Qiang Su, J. Phys. Chem. Solids 68 (2007) 1745.
[4] O.V. Solovyev, B.Z. Malkin, J. Mol. Struct. 838 (2007) 176.
[5] Kazuyoshi Ogasawara, Shinta Watanabe, Hiroaki Toyoshima, Mikhail G. Brik, Handbook on the Physics and Chemistry of Rare Earths, vol. 37 (2007) p. 1.
[6] Chaoshu Shi, Junyan Shi, Jie Deng, Zhengfu Han, Yinxue Zhou, Guobin Zhang, J. Electron Spectrosc. Relat. Phenom. 79 (1996) 121.
[7] M.N. Popova, J. Magn. Magn. Mater. 321 (2009) 716.
[8] Yun-Jeong Bae, Kyung-Hee Lee, Song-Ho Byeon, J. Lumin. 129 (2009) 81.
[9] Lei Zhou, Bing Yan, J. Phys. Chem. Solids 69 (2008) 2877.
[10] Yanlin Huang, Chuanfang Jiang, Yonggang Cao, Liang Shi, Hyo Jin Seo, Mater. Res. Bull. 44 (2009) 793.
[11] Tsuyoshi Kijima, Tomohiro Shinbori, Masami Sekita, Masafumi Uota, Go Sakai, J. Lumin. 128 (2008) 311.
[12] H. Kharbache, R. Mahiou, P. Boutinaud, D. Boyer, D. Zakaria, P. Deren, Opt. Mater. 31 (2009) 558.
[13] G. Bhaskar Kumar, S. Buddhudu, Ceram. Int. 35 (2009) 521.
[14] G. Seeta Rama Raju, S. Buddhudu, Physica B 403 (2008) 619.
[15] Ritwika Chakrabarti, Maumita Das, B. Karmakar, K. Annapurna, S. Buddhudu, J. Non-Cryst. Solids 353 (2007) 1422.
[16] C.H. Kam, S. Buddhudu, Physica B 344 (2004) 182.
[17] L.F. Edge, D.G. Scholm, S.A. Chambers, E. Cicerrella, J.L. Freeout, B. Hollander, J. Schubert, Appl. Phys. Lett. 84 (2004) 726.
[18] U. Schwingenschlögl, C. Schuster, Chem. Phys. Lett. 467 (2009) 354.
[19] S. Thiel, G. Hammerl, A. Schmehl, C.W. Schneider, J. Mannhart, Science 313 (2006) 1942.
[20] Chia-Liang Kuo, Yen-Hwei Chang, Moo-Chin Wang, Ceram. Int. 35 (2009) 327.
[21] Hussein Mortada, Mickael Derivaz, Didier Dentel, Jean-Luc Bischoff, Thin Solid Films 517 (2008) 441.
[22] Vijay Singh, D.T. Naidu, R.P.S. Chakradhar, Y.C. Ratnakaram, Jun-Jie Zhu, Manish Soni, Physica B 403 (2008) 3781.
[23] Przemysław J. Dereń, Rachid Mahiou, Philippe Goldner, Opt. Mater. 31 (2009) 465.
[24] Vijay Singh, T.K. Gundu Rao, J. Solid State Chem. 181 (2008) 1387.
[25] Vijay Singh, R.P.S. Chakradhar, J.L. Rao, Dong-Kuk Kim, J. Solid State Chem. 180 (2007) 2067.
[26] J.J. Kingsley, K.C. Patil, Mater. Lett. 6 (1988) 427.
[27] S. Cimino, L. Lisi, S. De Rossi, M. Faticanti, P. Porta, Appl. Catal., B 43 (2003) 397.
[28] P.J. Dereń, J.C. Krupa, J. Lumin. 102–103 (2003) 386.
[29] D. Hreniak, W. Strek, P. Dereń, A. Bednarkiewicz, A. Łukowiak, J. Alloys Compd. 408 (2006) 828.
[30] Zhi-yong Mao, Da-jian Wang, Qi-fei Lu, Wen-hui Yu, Zhi-hao Yuan, Chem. Commun. (2009) 346.
[31] G. Blasse, B.C. Grambier, Luminescent Materials. Springer-Verlag, Berlin, 1994, 43.
[32] R. Chen, J. Electrochem. Soc. 116 (1969) 1254.
[33] R.C. Weast (Ed.), Handbook of Chemistry and Physics, CRC, Cleveland, 1971.
[34] N.Y. Konstantinov, L.V. Karaseva, V.V. Gromov, Dokl. Acad. Nauk SSR 228 (1980) 631.
[35] V.T. Gritsyna, V.A. Kobyakov, Zh. Tekh. Fiz. 55 (1985) 354;
[, Sov. Phys. Tech. Phys. 30 (1985) 206].
[36] B. Dhabekar, E.A. Raja, S. Menon, T.K. Gundu Rao, R.K. Kher, B.C. Bhatt, J. Phys. D: Appl. Phys. 41 (2008) 115414.
[37] Sanjeev Menon, Bhushan Dhabekar, E. Alagu Raja, S.P. More, T.K. Gundu Rao, R.K. Kher, J. Lumin. 128 (2008) 1673.
[38] C.A. Hutchison, Phys. Rev. 75 (1949) 1769.
[39] M.G. Jani, R.B. Bossoli, L.E. Halliburton, Phys. Rev. B 27 (1983) 2285.